Korean J Biol Sci 7: 237-248, 2003

Organization of Projections from the Medial Temporal Cortical Areas to the Ventral Striatum in Macaque Monkeys

Yongwook Jung* and Sungwon Hong[1]

Department of Anatomy and [1]Department of Physiology, School of Medicine
Dongguk University, Kyungju 780-714, Korea

Key Words:

Ventral striatum
Entorhinal cortex
Perirhinal cortex
Parahippocampal cortex
Monkey
Retrograde tracing

Recent evidence on behaviors in macaque monkeys indicate that the medial temporal cortical areas such as the entorhinal cortex (EC), perirhinal cortex, and parahippocampal cortex (PHC) are importantly involved in limbic and sensory memory function. Neuroanatomical studies also have demonstrated that the medial temporal cortical areas are connected with the ventral striatum, although comparatively little is known about the precise topography of these connections. We investigated the topographic organization of connections between the medial temporal cortical areas and the ventral striatum by placing retrograde tracers into five different regions of the ventral striatum: the ventromedial caudate nucleus, ventral shell, central shell, dorsal core of the nucleus accumbens (NA), and ventrolateral putamen. We found that the shell of the NA was the main projection site from the medial temporal cortical areas. Within the shell of the NA, there were also differential connections: EC diffusely innervates shell of the NA, while the projections from the perirhinal cortex and PHC concentrate on the ventral shell of the NA. Taken together, it is possible that the ventral shell of the NA is the main integration site of the limbic and sensory memory coming from the EC, perirhinal cortex, and PHC.

The ventral striatum has been shown to play an important role in reward and goal-directed behaviors in primates (Burns et al., 1996; Robbins and Everitte, 1996). Previous studies also showed that these behaviors are associated with the convergent inputs from a wide range of cortical and subcortical areas, including the orbitomedial prefrontal cortex (OMPFC), amygdala, and ventral tegmental area (VTA) (Kunishio and Haber, 1994; Lynd-Balta and Haber, 1994; Gimnez-Amaya et al., 1995; Haber et al., 1995). However, it has not been known whether there are direct projections to the ventral striatum from the hippocampal formation (HF) and the medial temporal cortical areas including the entorhinal cortex (EC), perirhinal cortex, and parahippocampal cortex (PHC).

The EC constitutes a principal source of cortical inputs to the HF (Insausti et al., 1987a; Suzuki and Amaral, 1994), although the EC, itself, also receives inputs from many other cortical areas. The rostral and caudal portions of the EC are involved in different functions (Burwell and Amaral, 1998b; Naber et al., 2001). For example, the rostral EC receives olfactory and gustatory information, while the midcaudal EC is closely associated with the visuospatial circuit. In addition, the perirhinal cortex (areas 35 and 36) and PHC (areas TF and TH) also contribute the principal inputs to the EC (Suzuki and Amaral, 1994; Burwell and Amaral, 1998a). These cortical association areas receive convergent unimodal and polymodal sensory information from the temporal cortical areas in the superior temporal sulcus (STS) (Witter et al., 2000). The more rostrally located perirhinal cortex is involved in visual recognition, while the more caudal PHC contributes to visuospatial functions (Aggleton, 1995; Burwell and Amaral, 1998b). Of particular interest is that the most rostral region of the perirhinal cortex (the temporal polar region) is involved in social and emotional behavior in monkey (Stefanacci et al., 1996).

In primates, the ventral striatum includes the nucleus accumbens (NA) as well as the adjacent ventral caudate nucleus and putamen. The NA can be further divided into the shell and core (Heimer and Wilson, 1975; Kelley et al, 1982; Haber et al., 1990; Kunishio and Haber, 1994). In detail, the ventromedial part of the ventral striatum (VMS) includes both the medial caudate nucleus and the shell of NA sharing afferent inputs from specific regions of the OMPFC, amygdala, and VTA (Haber and McFarland, 1999). However, little is known about how these inputs are related to the afferent projections from the medial temporal cortical areas.

The aim of this study is to 1) determine relative contribution of inputs from the medial temporal cortical

*To whom correspondence should be addressed.
Tel: 82-54-770-2404, Fax: 82-54-770-2447
E-mail: jungyw@dongguk.ac.kr

areas to the ventral striatum; and 2) compare the topographic and laminar organizations of the projections from rostral and caudal regions of the medial temporal cortices, given their functional diversity. For this purpose, we injected retrograde tracers into different regions of the ventral striatum. We subdivided the ventral striatum into three areas: VMS, dorsal core, and ventrolateral putamen. The VMS was further subdivided into three areas: the ventromedial caudate nucleus, and the ventral and central shells of the NA.

Material and Methods

Retrograde tracing study

Seven adult Macaque monkeys (*Macacca nemestrina*) were used in these experiments. Initial anesthesia was administered by an intramuscular injection of ketamine (10 mg/kg). A deep surgical level of anesthesia was maintained by intravenous injection of phenobarbital (initial dose, 20 mg/kg, i.v. and maintained as needed). Temperature, heart rate, and respiration were monitored throughout the surgery. After monkeys were placed in a Kopf stereotaxic apparatus, a midline scalp incision was made and then muscle and fascia were displaced laterally to expose the skull. A craniotomy (2-3 cm^2) was made over the region of interest, and small dural incisions were made only at recording or injection. Electrophysiological mapping was performed to locate appropriate injection sites as described earlier (Haber et al., 1990). Retrograde tracers, wheat germ agglutinin conjugated to horseradish peroxidase (WGA-HRP) (40-50 nl, 4%; Sigma, St. Louis, MO) or Lucifer yellow (LY) conjugated to dextran amine (20-40 nl, 10%; Molecular Probes, Eugene, OR), were pressure-injected over 10 min into discrete regions of the ventral striatum using a 0.5 µl Hamilton syringe. After the injection, the syringe remained in place for 20 min to prevent leakage up into the needle track. After finishing tracer injections, the wound was closed in layers. The monkeys were again deeply anesthetized 10-12 days after the surgery with phenobarbital and perfused with saline followed 4% paraformaldehyde solution containing 1.5% sucrose in 0.1 M phosphate buffer, pH 7.4. The brains were cryoprotected in increasing gradients of sucrose (10, 20, and finally 30%). Serial sections (50 µm) were cut on a sliding microtome and put into 0.1 M phosphate buffer or stored in a cryoprotectant solution.

Immunocytochemical stain

We used immunocytochemical techniques to visualize the tracer. Before incubation with primary antiserum, the tissue was incubated in a solution containing 10% methanol and 3% H_2O_2 in 0.1 M phosphate buffer to inhibit endogenous peroxidase, followed by extensive rinsing with 0.3% Triton X-100 in 0.1 M phosphate buffer (PB-T), pH 7.4. Sections to be immunoreacted with anti-LY (Molecular Probes) or anti-WGA (Sigma) serum were then preincubated for 30 min in 10% normal goat serum (NGS) diluted with PB-T (NGS-PB-T). The tissue was placed in the primary antiserum, anti-LY diluted 1:1000 or anti-WGA-HRP diluted 1:2000 in NGS-PB-T for four nights at 4°C. Avidin-biotin reaction (rabbit Vectastain ABC kit; Vector Laboratories, Burlingama, CA) was used to visualize the LY and WGA. The tissue was rinsed in PB-T before incubating in biotinylated goat anti-rabbit 1:400 NGS-PB-T at room temperature for 45 min. After rinsing, the tissue was incubated in the rabbit avidin-biotin complex (1:200) at room temperature for 1 hr. Antisera binding was visualized by incubating the tissue for 10-12 min in a solution of 0.05% 3,3'-diaminobenzidine tetrahydrochloride (DAB) and 0.01% H_2O_2 in 0.5 M Tris buffer. For intensified staining, the tissues were rinsed several times and then treated with 0.025% cobalt chloride and 0.02% nickel ammonium sulfate to yield a black reaction product. After thorough rinsing, sections were mounted onto gel-coated slides and counterstained with cresyl violet using a standard Nissl procedure.

Charting

Retrogradely labeled cells in the medial temporal cortical areas were charted using a light microscope fitted with a drawing tube. With the aid of a drawing tablet, charts were traced into a Power Macintosh computer to create composite images. The nomenclature and abbreviations used are those that have been employed in the Rhesus monkey brain in stereotaxic coordinates (Paxinos et al., 2000). Using Nissl-stained coronal section, we determined the boundaries of cytoarchitetonic subdivisions of the EC as described by Amaral et al. (1987). The rostral subdivisions of EC (EO1 and ER) in the monkey tend to be less laminated and roughly corresponds to the lateral EC of the rat. The intermediate (EI) and caudal regions (ECC and ECL) of the EC are organized in a more columnar and laminar fashion and would correspond to the medial portion of the rat EC. The nomenclature and boundaries of the perirhinal cortex and PHC analyzed in this study are similar to those used previously (Suzuki and Amaral, 1994). The perirhinal cortex is composed of a smaller, medially situated area 35 and a larger, laterally situated area 36. The most rostral portion of area 35 is located on the temporal pole, named as a temporal polar region. There are three subdivisions of area 36: 36R, 36, 36O. The PHC is caudally adjacent to both EC and the perirhinal cortex. It is made up of a smaller, medially situated area TH and a larger, laterally situated area TF.

Abbreviations

35, 36R, areas of perirhinal cortex; amt, anterior middle

temporal sulcus; EC, entorhinal cortex; ECC, caudal entorhinal cortex; ECL, caudal limited entorhinal cortex; EI, intermediate entorhinal cortex; ELC, lateral, caudal entorhinal cortex; ELR, lateral, rostral entorhinal cortex; EO1, olfactory part of entorhinal cortex; ER, rostral entorhinal cortex; hf, hippocampal fissure; HF, hippocampal formation; NA, nucleus accumbens; OMPFC, orbitomedial prefrontal cortex; ots, occipitotemporal sulcus; PHC, parahippocampal gyrus; Pu, putamen; rf, rhinal fissure; RS, rhinal sulcus; STS, superior temporal sulcus; TF, area TF of parahippocampal gyrus; TFL, lateral TF area of parahippocampal gyrus; TFm, medial TF area of parahippocampal gyrus; TFO, occipital TF area of parahippocampal gyrus; TH, area TH of parahippocampal gyrus; THO, occipital TH area of parahippocampal gyrus; VMS, ventromedial part of ventral striatum; VTA, ventral tegmental area.

Results

Tracer injections in the ventral striatum

Total of seven injections were made in four different

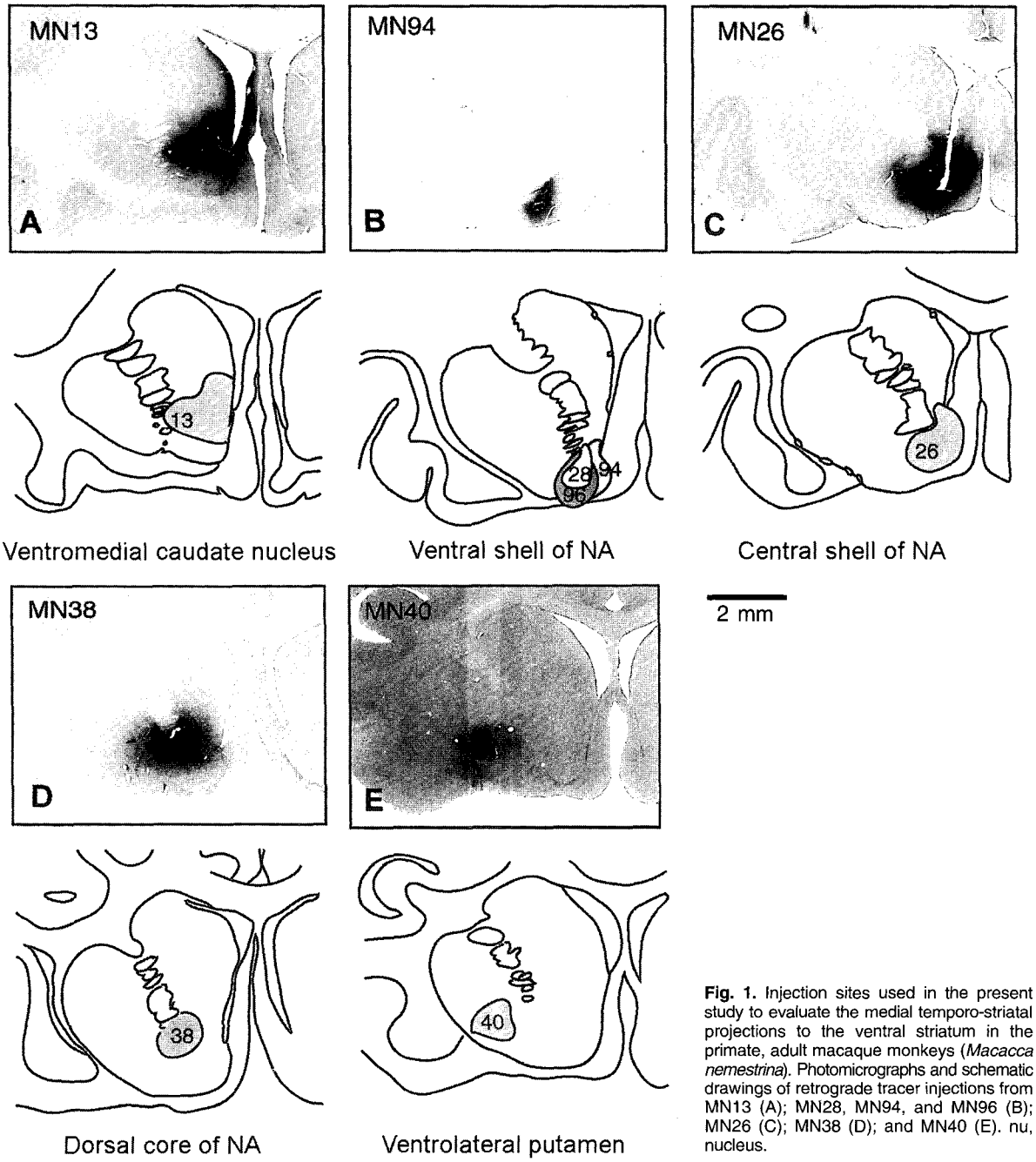

Fig. 1. Injection sites used in the present study to evaluate the medial temporo-striatal projections to the ventral striatum in the primate, adult macaque monkeys (*Macacca nemestrina*). Photomicrographs and schematic drawings of retrograde tracer injections from MN13 (A); MN28, MN94, and MN96 (B); MN26 (C); MN38 (D); and MN40 (E). nu, nucleus.

Table 1. Summary of retrogradely labeled cells in medial temporal cortical areas

Medial temporal cortical regions	Ventral Striatal Injection Sites				
	Ventromedial caudate nu	*Ventral shell* of NA	*Central shell* of NA	*Dorsal core* of NA	Ventrolateral Pu
EO1	-	+	++++	-	-
ELR	-	++++	-	-	+
ER	-	+	+++	+	-
EI	++	++++	++++	-	-
ELC	+	++++	+	-	-
ECC	-	++++	++++	-	+
ECL	++	++++	++++	-	-
35	++	++++	+	++	+
36	+	++++	+	+	+
TF	-	+++	-	+	-
TH	++	++++	+	-	+
TFM	-	+	-	-	-
TFL	-	-	-	-	-
THO	-	-	-	-	-
TFO	-	-	-	-	-

This summary is based on relative densities of retrogradely labeled neurons in each of the specific regions of the medial temporal cortical regions as seen in the representative drawings, where - represents no retrogradely labeled cells observed and + to ++++ represent increasing relative densities from occasional cells to very dense labeling. Each of the cases has a different number of representative drawings. Thus, the relative densities of retrogradely labeled neurons in each case are weighted accordingly for more accurate comparison with the other cases. Entorhinal cortex (EC) includes the areas from EO1 to ECL. Perirhinal cortex includes the areas 35 and 36. Parahippocampal cortex includes the areas from TF to TFO. nu, nucleus.

parts of the ventral striatum, as shown in Fig. 1. One injection was placed in the ventromedial caudate nucleus (case MN13). Four injection sites were located in the shell of NA; three in the ventral shell of the NA (cases MN28, MN94, and MN96) and one in the central shell of the NA (Case MN26). Another site was centered in the dorsal core of the NA (Case MN38) and the final one laterally into the ventrolateral putamen (Cases MN 40).

Distribution and topography of retrogradely labeled cells

The medial temporal cortical areas including EC, perirhinal cortex, and PHC were labeled after all ventral striatal injections (Table 1). The extent and distribution of labeling were different depending on the location and injection sites. However, all labeled cells found in these areas are ipsilateral to the injection site. The major differences in labeling patterns following injections into different parts of the ventral striatum concerned with the rostrocaudal position of cells. The laminar organization of labeled cells was similar for all the injection sites to the extent that the majority of labeled cells are present in the deep layers V and VI throughout the rostrocaudal extent of the medial temporal cortex, although some labeled cells were also located in layer III.

Projections to the ventromedial part (VMS) of the ventral striatum

Projections to the ventromedial caudate nucleus
(Case MN13)

Most of HRP-labeled cells were seen in the midcaudal two-thirds of the EC, from EI to ECL (Fig. 2). Moderate numbers of labeled cells were found in the EI, whereas in more caudal portions relatively small numbers of labeled cells were seen in the ECL (Fig. 2B-D). Scattered labeled cells were also seen in the ELC, which occupied the medial bank of the rhinal sulcus (RS) (Fig. 2B). However, the rostral one-third of the EC including EO1 and ER contained no labeled cells. In the perirhinal cortex, a moderate population of HRP-labeled cells was found in the most rostral level of area 35 (temporal polar portion), which was located in the fundus and lateral bank of the RS (Fig. 2A). Small numbers of labeled cells were observed in areas 35 and 36R (Fig. 2B, D). Caudally, there was a light distribution of HRP-labeled cells in area 36 (Fig. 2E). The area TH of the PHC contained moderate numbers of labeled cells (Fig. 2E). Thus, the monkey medial temporal cortical areas contribute relatively little cortical input to the ventromedial caudate nucleus.

Projections to the ventral shell of the NA
(Cases MN28, MN94, and MN96)

Case MN28 (Fig. 3). The HRP-labeled cells after injection to the ventral shell of the NA was denser than those seen after injections into the ventromedial caudate nucleus. In the EC, denser HRP-labeled cells was observed in the midcaudal two-thirds (EI to ECC) than in the rostral one-third. At the midcaudal two-thirds, the highest number of labeled cells was found in the medial portion (EI and ECC) as well as the medial bank (ELC)

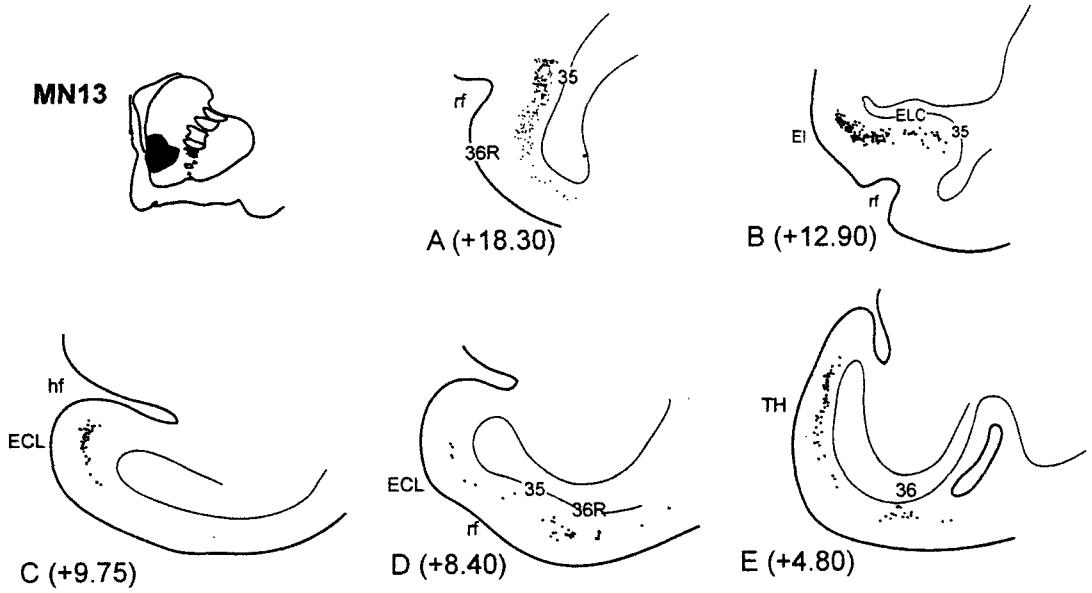

Fig. 2. Schematic drawings illustrating the distribution of the retrogradely labeled cells in the different levels of the entorhinal cortex (EC), perirhinal cortex, and parahippocampal cortex (PHC) after HRP injections placed in the ventromedial caudate nucleus (Case MN13). Numbers next to labels indicate approximate AP (anteroposterior) level, relative to interaural zero.

of the RS (Fig. 3B-D). Fewer labeled cells were seen in the rostral one-third than in the caudal two-thirds. A small number of labeled cells were seen in EO1. In addition to EO1, ELR in the medial bank of the RS also contained scattered labeled cells (Fig. 3A). In the perirhinal cortex, the highest number of HRP-labeled cells was evenly distributed in areas 35 and 36R (Fig. 3A-E). In area 35, the highest concentration of the labeled cells was found in the temporal polar portion of the RS. The dense HRP-labeled cells in area 36R gradually decreased toward the caudal level (Fig. 3E). Within the PHC, the medial TH contained the highest number of HRP-labeled cells (Fig. 3E). However, there were small numbers of labeled cells in the area TF, which was located in the

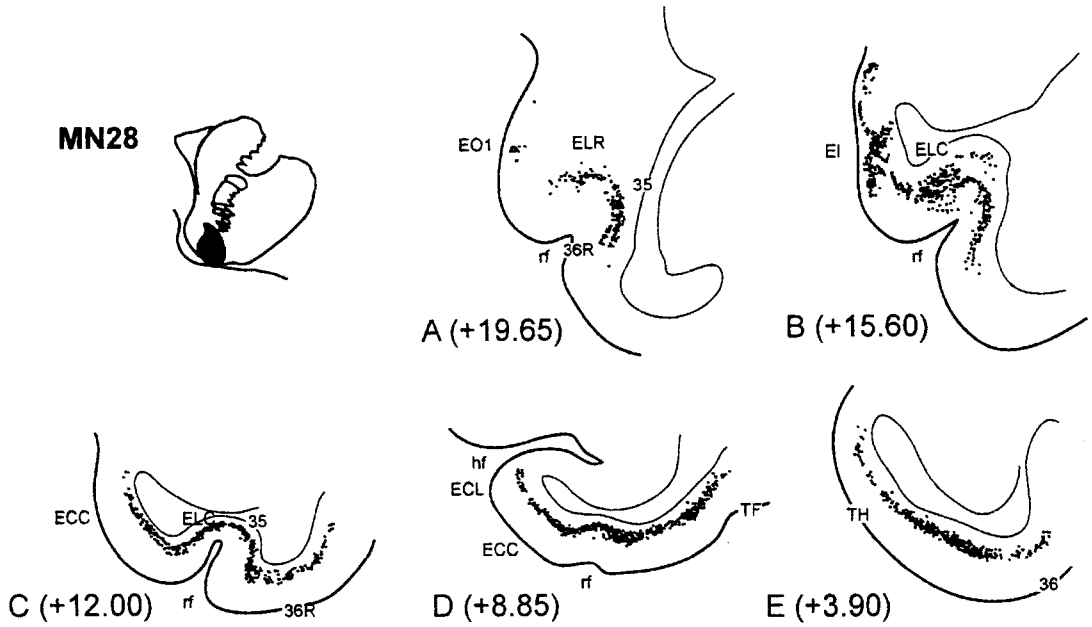

Fig. 3. Schematic drawings illustrating the distribution of the retrogradely labeled cells in the different levels of the EC, perirhinal cortex, and PHC, after HRP injections placed in the ventral shell of the NA (Case MN28). Numbers next to labels indicate approximate AP level, relative to interaural zero.

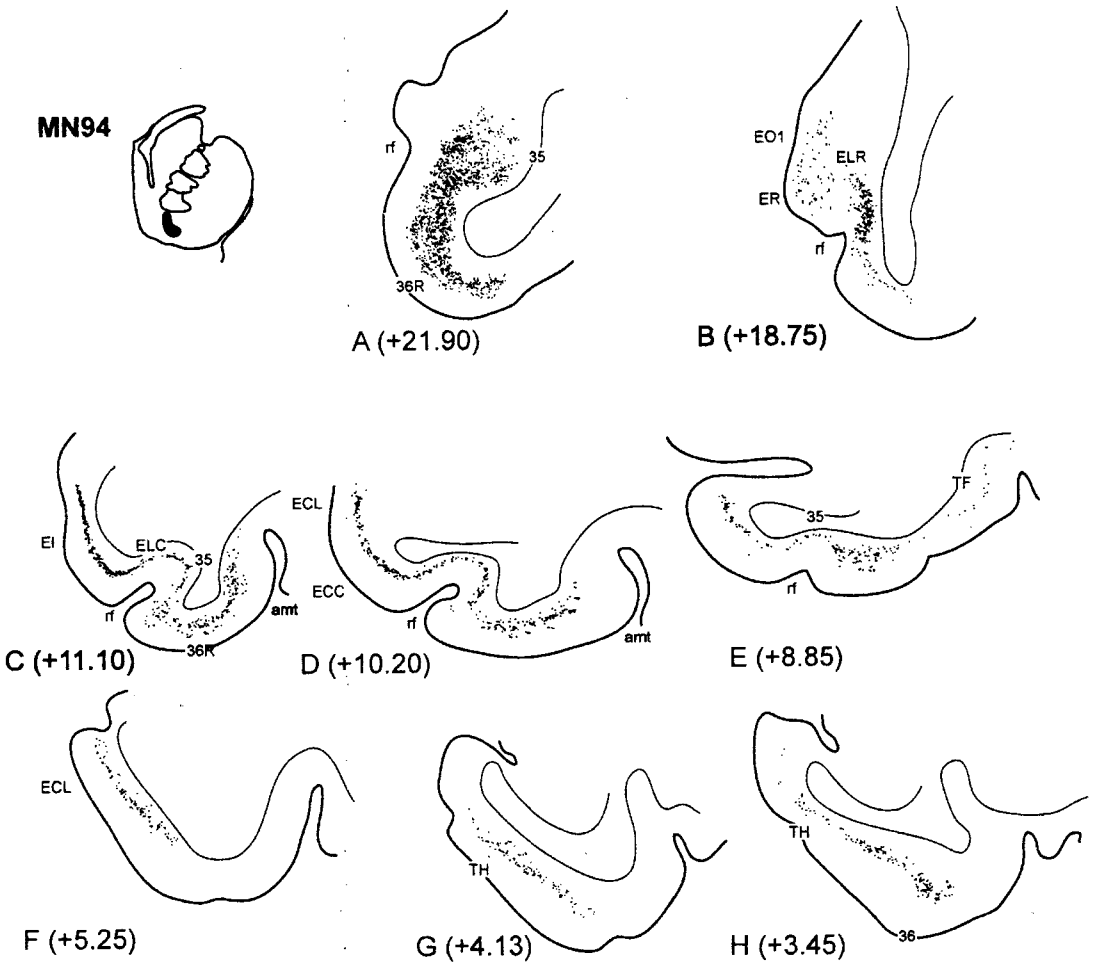

Fig. 4. Schematic drawings illustrating the distribution of the retrogradely labeled cells in the different levels of the EC, perirhinal cortex, and PHC, after HRP injections placed in the ventral shell of the NA (Case MN94). Numbers next to labels indicate approximate AP level, relative to interaural zero.

lateral part of the PHC (Fig. 3D). Most of the labeled cells in the EC, perirhinal cortex, and PHC were distributed in layers V and VI.

Case MN94 (Fig. 4). In the EC, a dense group of labeled cells was seen in the midcaudal two-thirds compared to the rostral one-third. EI, ECC, and ECL in the medial portions of the RS contained the highest number of HRP-labeled cells (Fig. 4B-F). A small number of labeled cells was also seen in the medial bank (ELC) of the RS at the middle level (Fig. 4C-E). However, the EO1 and ER at the rostral level contained a few labeled cells. The HRP-labeled cells in the EO1 and ER were scattered (Fig. 4B). The greatest concentration of HRP-labeled cells was seen in the temporal polar portion of the perirhinal cortex (Fig. 4A). A relatively high concentration of labeled cells was observed in areas 35 and 36R (Fig. 4B-E). The majority of the HRP-labeled cells was concentrated in the area TH, the medial part of the PHC (Fig. 4G-H). A few labeled cells were also found in the lateral TF (Fig. 4E). The labeled cells in the EC, perirhinal cortex and PHC were mainly located in layers V and VI.

Case MN96 (Fig. 5). In the EC, a large number of densely HRP-labeled cells were found in the midcaudal two-thirds. This finding was similar to cases 28 and 94, where a dense concentration of labeled cells was seen in the EI to ECL (Fig. 5B-F). At the rostral level, the ER contained a moderate number of labeled cells (Fig. 5A). More rostrally, the EO1 contained a few labeled cells, which are scattered (Fig. 5A). Few to moderate numbers of labeled cells were observed in the rostral EC following injections into the ventral region of the shell. This case was in contrast to medial injection case MN13, where no cells were seen in the rostral EC. The temporal polar portion of the perirhinal cortex had the highest number of HRP-labeled cells like previous ventral shell injection cases (Fig. 5A). Areas 35 and 36R still had a significant number of labeled cells (Fig. 6B-F). Moderate numbers of labeled cells were located in the area TF (Fig. 5E-F). There were many labeled cells present in the area TH (Fig. 5G). These findings in the PHC were similar to

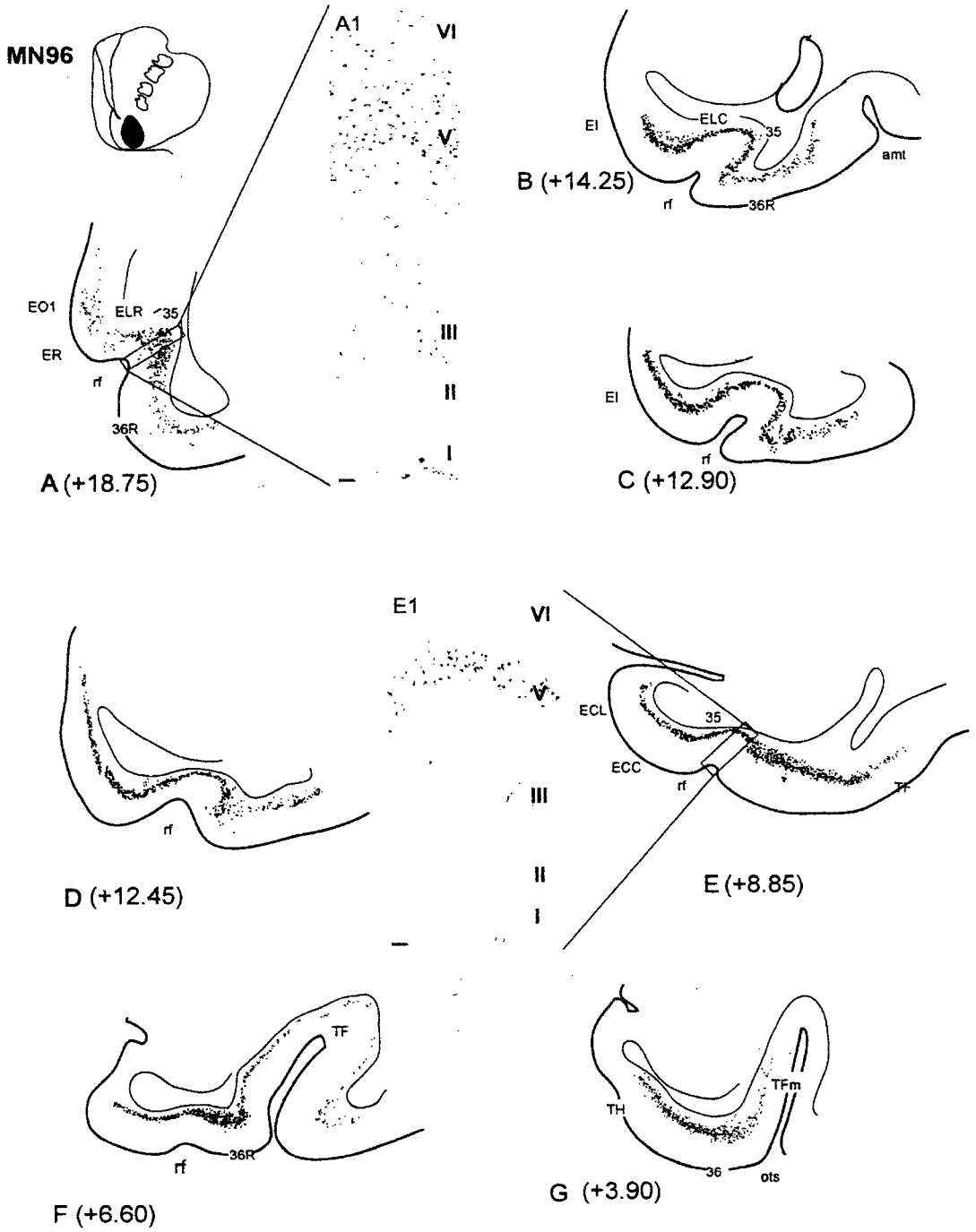

Fig. 5. Schematic drawings illustrating the distribution of the retrogradely labeled cells in the different levels of the EC, perirhinal cortex, and PHC, after HRP injections placed in the ventral shell of the nucleus accumbens (NA) (case MN96). *Inset* A1: labeled cells at the temporal polar region are found in layers III, V, and VI of the six-layered temporal cortex. *Inset* E1: however, labeled cells at the caudal level of the area 35 are localized in layer V. Scale bar=50 μm. Numbers next to labels indicate approximate AP level, relative to interaural zero.

previous ventral shell injection cases. Occasionally, labeled cells were also found in the area TFm, the caudal part of area TF (Fig. 5G). Although some HRP-labeled cells in the temporal polar portion of the area 35 were located in layer III, most of the labeled cells were located in layers V and VI (Fig. 5A, *Inset* A1). Toward the caudal levels, most labeled cells in area 35 were concentrated in layer V (Fig. 5E, *Inset* E1). These findings from all three injection cases demonstrates that the medial temporal cortical areas constitutes a major source

of cortical input to the ventral shell of NA.

Projections to the central shell of the NA
(Case MN26)

After HRP injection into the central shell of the NA, dense labeling was seen throughout the rostrocaudal extent of the EC (Fig. 6). A large number of HRP-labeled cells were found in the rostral EO1 and ER (Fig. 6A). This finding was in contrast to the ventral shell injection cases, where a small number of the labeled cells were seen in the EO1 and ER (Fig. 3A and 4B). The inter-

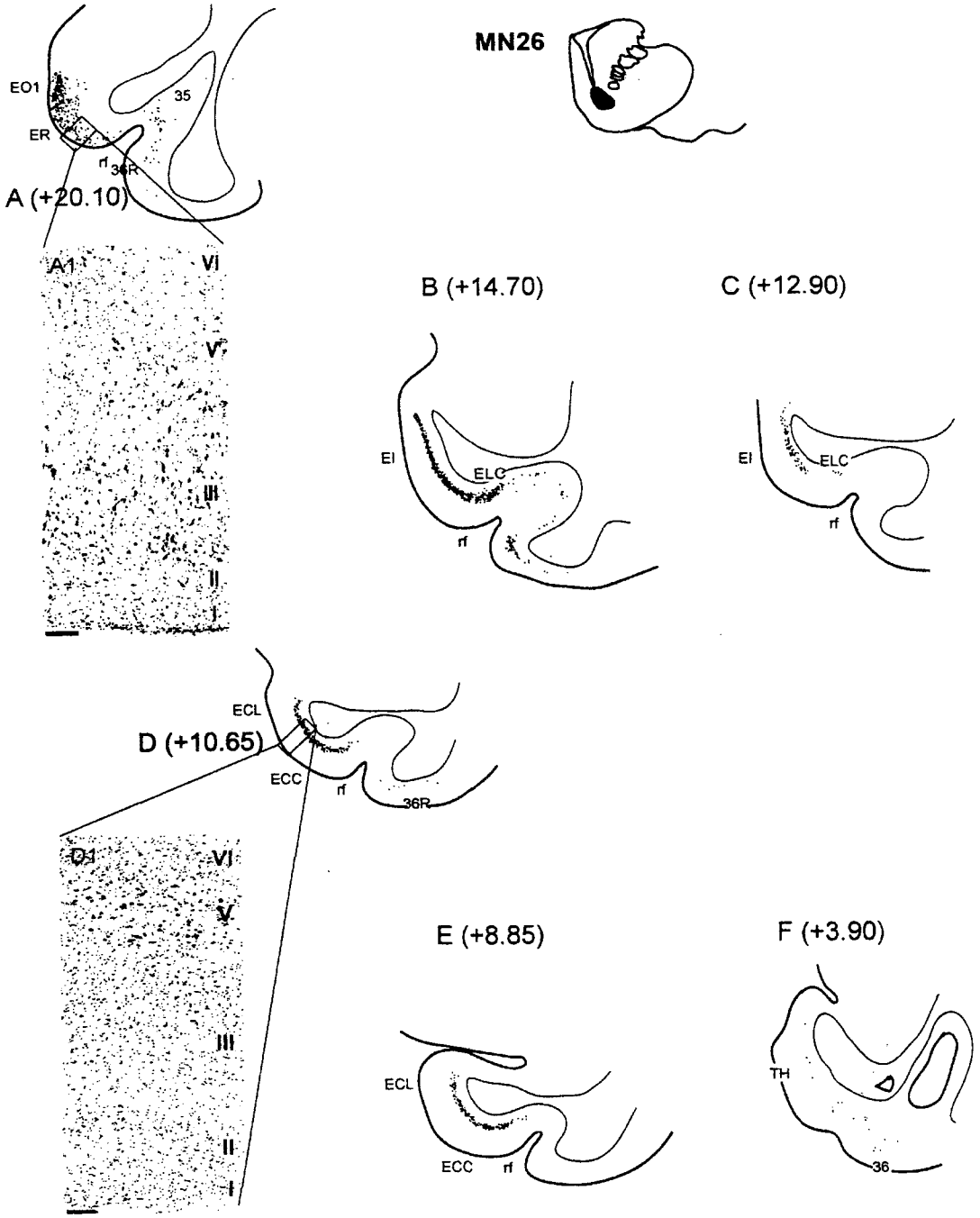

Fig. 6. Schematic drawings illustrating the distribution of the retrogradely labeled cells in the different levels of the EC, perirhinal cortex, and PHC, after HRP injections placed in the central shell of the NA (case MN26). *Inset* A1: labeled cells at the rostral level of the EC (ER) are found in layers III and V of the six-layered cortex. *Inset* D1: labeled cells at the caudal level of the EC (ECC) are localized in layer V. Scale bar=50 μm. Numbers next to labels indicate approximate AP level, relative to interaural zero.

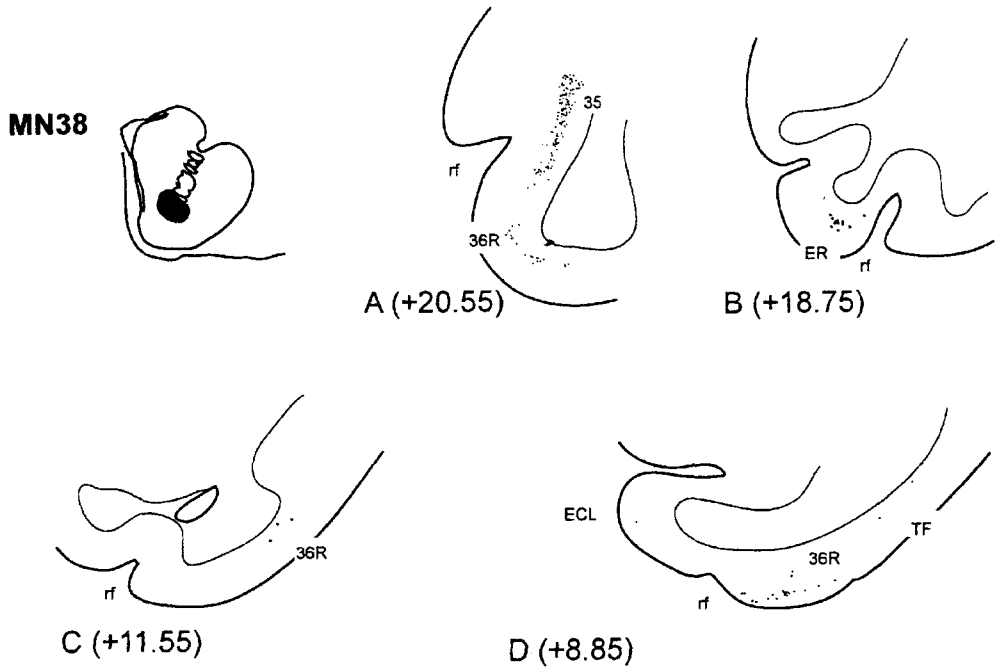

Fig. 7. Schematic drawings illustrating the distribution of the retrogradely labeled cells in the different levels of the EC, perirhinal cortex, and PHC after LY injections placed in the dorsal core of the NA (case MN38). Numbers next to labels indicate approximate AP level, relative to interaural zero.

mediate and caudal portions of the EC contained many labeled cells (Fig. 6B-E). The concentration of labeled cells in the perirhinal cortex and PHC was less than that seen after injections into the ventral shell. Fewer cells were labeled in the areas 35 and 36R (Fig. 6A-F). The area TH of the PHC also contained a few labeled cells,

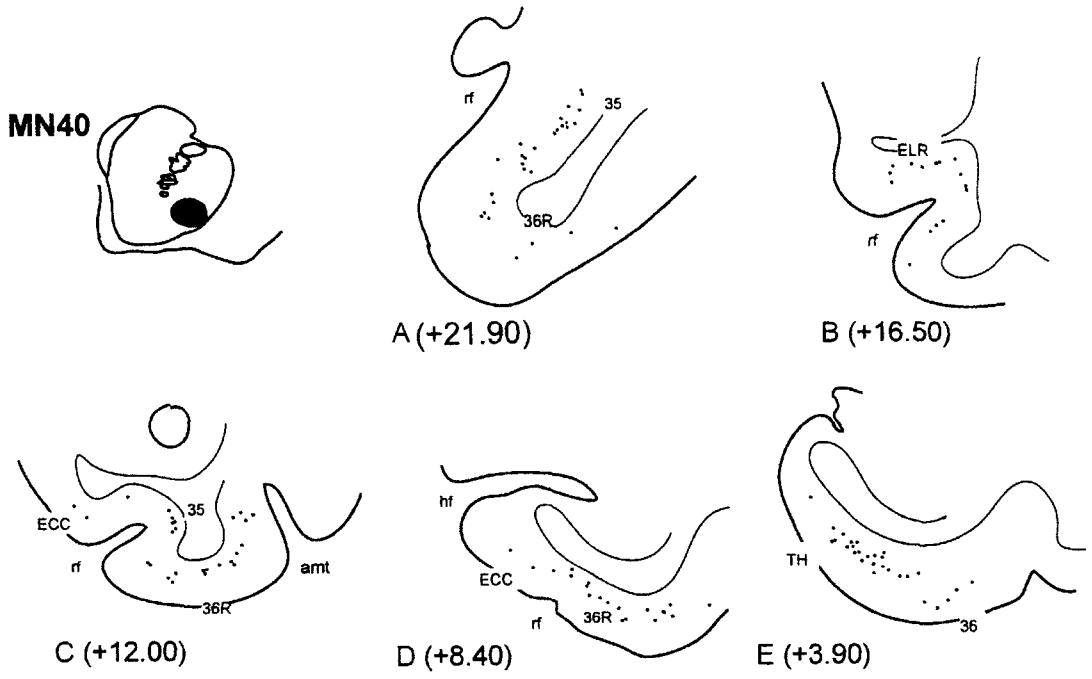

Fig. 8. Schematic drawings illustrating the distribution of the retrogradely labeled cells in the different levels of the EC, perirhinal cortex, and PHC, after LY injections placed in the ventrolateral putamen (case MN40). Numbers next to labels indicate approximate AP level, relative to interaural zero.

but there were no labeled cells in the TF of the PHC (Fig. 6F). These findings were in contrast to ventral shell injection cases, where the densest labeled cells were seen in the perirhinal cortex and PHC. The labeled cells in the ER were distributed in layers III to V (Fig. 6A, *Inset* A1), whereas the labeled cells in the ECC confined to the layers V and VI (Fig. 6D, *Inset* D1). Thus, these results also strongly supports the notion that the EC constitutes a major source of cortical input to the central shell of NA.

Projections to the dorsal core of the NA
(Case MN38)

Of all the cases, this case contained the fewest number of LY-labeled cells in the EC (Fig. 7). A few scattered LY-labeled cells were observed in the rostral one-third (ER). There were moderate numbers of the labeled cells in the temporal polar portion of the perirhinal cortex (Fig. 7A). No labeled cells were observed in the area 35 (Fig. 7B). In addition, there were few labeled cells seen in the area 36R (Fig. 7C-D). Occasionally, labeled cells were seen in the area TF of the PHC (Fig. 7D). These results indicate that the medial temporal cortical areas are not major sources of cortical input to the dorsal core of NA.

Projections to the ventrolateral putamen
(Case MN40)

There were a few LY-labeled cells in the ELR and ECC (Fig. 8). In the perirhinal cortex, moderate numbers of labeled cells were detected in the temporal polar portion whereas a few labeled cells were observed in area 36R (Fig. 8A-D). In addition, a few labeled cells were also found in the TF of the PHC (Fig. 8D). These results also indicate that the medial temporal cortical areas do not mainly contribute the cortical input to the ventrolateral putamen.

Discussion

Cortical input to the ventral striatum

The present study demonstrates that the main projections from the EC, the perirhinal cortex, and the PHC terminate in the shell of NA. In contrast, there are significantly fewer projections to the ventromedial caudate nucleus, dorsal core of the NA and the ventrolateral putamen of the ventral striatum. Within the shell of the NA, there are also differential connections: EC mainly innervates ventral shell and central shell of the NA, while the projections from the perirhinal cortex and the PHC concentrate in the ventral shell of the NA.

The possible roles of connections between the medial temporal cortical areas and the shell of NA

Direct projections from EC to the shell of NA

The olfactory portion of the rostral EC (EO1 and ER) receives direct sensory projections from the olfactory bulb and the piriform cortex (Insausti et al., 1987b) and then projects to the uncus of the HF (Insausti et al., 2002). Thus, the main projections from the rostral EC to the shell of the NA means that most of the olfactory information from the rostral EC is concentrated in the shell of the NA. In addition, the midcaudal EC connects with the retrosplenial, posterior parietal, prelimbic, and infralimbic cortices as well as pre- and parasubiculum, all of which are closely associated with visuospatial circuits for head direction (Swanson and Kohler, 1986; Suzuki and Amaral, 1994; Burwell and Amaral, 1998b). These findings suggest that the rostral and caudal EC are functionally segregated and their olfaction and visuospatial information is converged into the shell of the NA.

Direct projections from the temporal polar region and ventral shell of NA

Interestingly, the temporal polar region of the perirhinal cortex has stronger projections to the ventral shell of the NA compared to those from other portions of areas 35 and 36. Several previous studies have also demonstrated strong interconnections between the amygdala and temporal polar region (Aggleton et al., 1980; Moran et al., 1987; Stefanacci et al., 1996). The amygdala is also interconnected with the medial prefrontal cortex (Aggleton et al., 1980; Amaral and Price, 1984; Barbas and De Olmos, 1990; Carmichael and Price, 1995). Limited studies with lesions of the temporal polar region produced remarkable changes in social and emotional behavior in monkeys. In animals postoperatively returned to free-ranging conditions, for example, those with temporal polar lesions failed to return to their social group and showed decreased aggressiveness to other monkeys and humans (Myers and Swett, 1970; Kling and Steklis, 1976; Kling et al., 1993). Given the current understanding of the importance of interconnections between the temporal polar region, amygdala, and medial prefrontal cortex, these structures may form an anatomically interconnected network underlying the mediation of normal social interactions and the orchestration of appropriate species-specific responses (Kling and Steklis, 1976; Stefanacci et al., 1996). These results suggest that the limbic information associated with the social and emotional behavior in the temporal polar region of the perirhinal cortex specifically transfers to the ventral shell of the NA.

Direct projections from the perirhinal cortex (areas 35 and 36) and PHC to the ventral shell of NA

The main projections to the EC arise from the perirhinal

cortex and the PHC (Burwell and Amaral, 1998a; Witter et al., 2000; Naber et al., 2001). The perirhinal cortex specifically receives inputs from the unimodal and multimodal regions of the STS, lateral, orbital prefrontal, rostral temporal association cortex and caudal cingulate cortices which are thought to be preferentially involved in the visual recognition memory (Deacon et al., 1983; Burwell and Amaral, 1998a,b).

The PHC receives its primary input from caudal visual association areas, as well as visuospatial areas such as the inferior parietal lobe, retrosplenial, and posterior parietal cortices (Cavada and Goldman-Rakic, 1989; Wyss and Van Groen, 1992; Burwell and Amaral, 1998b). Other studies on parieto-hippocampal connections similarly emphasized dual pathways through the presubiculum and the PHC (Rockland and Van Hoesen, 1999). The PHC is also closely connected with the medial prefrontal cortex thought to be involved in the processing of visual and spatial information (Kesner et al., 1989; Aggleton, 1995; Burwell and Amaral, 1998b) suggesting that these regions themselves may contribute to visuospatial functions. In the present study, we showed projections from the perirhinal cortex and PHC were specifically directed to the ventral shell of the NA. Therefore, it is possible that the ventral shell of the NA is the main integration site of the visuospatial and visual recognition information coming from the perirhinal cortex and PHC.

Taken together, it is possible that the ventral shell of the NA is the main integration site of the limbic and sensory information coming from the medial temporal cortical areas (EC, perirhinal cortex, PHC).

Dual innervation to the ventral striatum from the infra- and supragranular layers

The projections from the EC, perirhinal cortex, and PHC to the ventral striatum arise primarily from cells in layers V or VI, and to a lesser extent from cells located in layer III. These results indicate that the main projections from the medial temporal lobe arise in infragranular layers. Previous studies have indicated that associational connections arise largely in infragranular layers (Witter and Amaral, 1991; Dolorfo and Amaral, 1998; Witter et al., 2000). Several studies also indicate that the cells in layers V and VI of the medial temporal cortical areas give rise to most of the nonhippocampal connections to widespread cortical and subcortical structures. In contrast, most neurons in layer III give rise to the perforant pathway which projects to all subfields of the HF (Steward and Scoville, 1976; Witter et al., 1989; Lingenhohl and Finch, 1991; Tamamaki and Noyjo, 1993). These findings indicate that the ventral striatum is dually innervated from an intrinsic hippocampal pathway in layer III and an extrinsic nonhippocampal pathway in layers V and VI.

Acknowledgements

This work was supported by Dongguk University Research Fund.

References

Aggleton JP, Burton MJ, and Passingham RE (1980) Cortical and subcortical afferents to the amygdala of the rhesus monkey (*Macaca mulatta*). *Brain Res* 190: 347-368.

Aggleton JP, Neave N, Nagle S, and Sahgal A (1995) A comparision of the effects of medial prefrontal, cingulate cortex, and cingulum bundle lesions on tests of spatial memory: evidence of a double dissociation between frontal and cingulum bundle contributions. *J Neurosci* 15: 7270-7281.

Amaral DG and Price JL (1984) Amygdalo-cortical projections in the monkey (*Macaca fascicularis*). *J Comp Neurol* 230: 465-496.

Amaral DG, Insausti R, and Cowan WM (1987) The entorhinal cortex of the monkey. I. Cytoarchitectonic organization. *J Comp Neurol* 264: 326-355.

Barbas H and De Olmos J (1990) Projections from the amygdala to basoventral and mediodorsal prefrontal regions in the rhesus monkey. *J Comp Neurol* 300: 549-571.

Burwell RD and Amaral DG (1998a) Perirhinal and postrhinal cortices of the rat: interconnectivity and connections with the entorhinal cortex. *J Comp Neurol* 391: 293-321.

Burwell RD and Amaral DG (1998b) Cortical afferents of the perirhinal, postrhinal and entorhinal cortices of the rat. *J Comp Neurol* 398: 179-205.

Burns LH, Annett L, Kelley AE, Everitt BJ, and Robbins TW (1996) Effects of lesions to amygdala, ventral subiculum, medial prefrontal cortex, and nucleus accumbens on the reaction to novelty: implication for limbic-striatal interactions. *Behav Neurosci* 110: 60-73.

Carmichael ST and Price JL (1995) Limbic connections of the orbital and medial prefrontal cortex in macaque monkey. *J Comp Neurol* 363: 642-664.

Cavada C and Goldman-Rakic PS (1989) Posterior parietal cortex in rhesus monkey: I. Parcellation of areas based on distinctive limbic and sensory corticocortical connections. *J Comp Neurol* 287: 393-421.

Deacon TW, Eichenbaum H, Rosenberg P, and Eckmann KW (1983) Afferent connections of the perirhinal cortex in the rat. *J Comp Neurol* 220: 168-190.

Dolorfo CL and Amaral DG (1998) Entorhinal cortex of the rat: Organization of intrinsic connections. *J Comp Neurol* 398: 49-82.

Gimenez-Amaya JM, McFarland NR, de las Heras S, and Haber SN (1995) Organization of thalamic projections to the ventral striatum in the primate. *J Comp Neurol* 354: 127-149.

Haber SN, Lynd E, Klein C, and Groenewegen HJ (1990) Topographic organization of the ventral striatal efferent projections in the rhesus monkey: an anterograde tracing study. *J Comp Neurol* 293: 282-298.

Haber SN, Kunishio K, Mizobuchi M, and Lynd-Balta E (1995) The orbital and medial prefrontal circuit through the primate basal ganglia. *J Neurosci* 15: 4851-4867.

Haber SN and McFarland NR (1999) The concept of the ventral striatum in nonhuman primates. *Ann N Y Acad Sci* 887: 33-48.

Heimer L and Wilson RD (1975) The subcortical projections of the allocortex: similarities in the neural associations of the hippocampus, the piriform cortex, and the neocortex. In: Santini M (Ed), Golgi Centennial Symposium: Perspectives in Neurobiology. Ravan, New York, pp 177-193.

Insausti R, Amaral DG, and Cowan WM (1987a) The entorhinal cortex of the monkey. II. Cortical afferents. *J Comp Neurol* 264: 356-395.

Insausti R, Amaral DG, and Crwan WM (1987b) The entorhinal cortex of the monkey: III. Subcortical afferents. *J Comp Neurol* 264: 356-395.

Insausti R, Marcos P, Arroyo-Jimenez M, Blaizot X, and Martine-Marcos A (2002) Comparative aspects of the olfactory portion of the entorhinal cortex and its projection to the hippocampus in rodents, nonhuman primates, and the human brain. *Brain Res Bull* 57: 5570-560.

Kelley AE, Domesick VB, and Nauta WJH (1982) The amygdalostriatal projection in the rat an anatomical study by anterograde and retrograde tracing methods. *Neuroscience* 7: 615-630.

Kesner RP, Farnsworth G, and DiMattia BV (1989) Double dissociation of egocentric and allocentric space following medial prefrontal and parietal cortex lesions in the rat. *Behav Neurosci* 103: 956-961.

Kling A and Steklis HD (1976) A neural substrate for affinitive behavior in nonhuman primates. *Brain Behav Evol* 12: 216-238.

Kling AS, Tachiki K, and Llovd R (1993) Neurochemical correlates of the Kluver-Bucy syndrome by in vivo microdialysis in monkey. *Behav Brain Res* 56: 161-170.

Kunishino K and Haber SN (1994) Primate cingulostriatal projection: Limbic striatal versus sensorimotor striatal input. *J Comp Neurol* 350: 337-356.

Lingenhohl K and Finch DM (1991) Morphological characterization of rat entorhinal neurones *in vivo*: soma-dendrtic structure and axonal domains. *Exp Brain Res* 84: 57074.

Lynd-Balta E and Haber SN (1994) The organization of midbrain projections to the ventral striatum in the primate. *Neuroscience* 59: 609-623.

Moran MA, Mufson EJ, and Mesulam MM (1987) Neural inputs into the temporopolar cortex of the rhesus monkey. *J Comp Neurol* 256: 88-103.

Myers RE and Swett C (1970) Social behavior deficits of free-ranging monkey after anterior temporal cortex of the removal: A preliminary report. *Brain Res* 18: 551-556.

Naber PA, Witter MP and Silva LD (2001) Evidence for a direct projection from postrhinal cortex to subiculum in the rat. *Hippocampus* 11: 105-117.

Paxinos G, Huang XF, and Toga AW (2000) The Rhesus Monkey Brain in Stereotaxic Coordinates. 2nd Ed. Academic Press, Sydney.

Rockland KS and Van Hoesen GW (1999) Some temporal and parietal cortical connections converge in CA1 of the primate hippocampus. *Cereb Cort* 9: 232-237.

Robbins TW and Everitt BJ (1996) Neurobehavioral mechanism of reward and motivation. *Curr Opin Neurobiol* 6: 228-236.

Stefanacci L, Suzuki WA, and Amaral DG (1996) Organization of connections between the amygdalod complex and the perirhinal and parahippocampal cortices in Macaque monkeys. *J Comp Neurol* 375: 552-582.

Steward O and Scoville SA (1976) Cells of origin of entorhinal cortical afferents to the hippocampus and fascia dentata of the rat. *J Comp Neurol* 169: 347-370.

Suzuki WA and Amaral DG (1994) Topographic organization of the reciprocal connections between the monkey entorhinal cortex and the perirhinal cortex and parahippocampal cortices. *J Neurosci* 14: 1856-1877.

Swanson LW and Kohler C (1986) Anatomical evidence for direct projections from the entorhinal area to the entire cortical mantle in the rat. *J Neurosci* 6: 3010-3023.

Tamamaki N and Nojyo Y (1993) Projection of the entorhinal layer II neurons in the rat as revealed by intracellular pressure-injection of neurobiotin. *Hippocampus* 3: 471-480.

Witter MP and Amaral DG (1991) Entorhinal cortex of the monkey: V. Projections to the dentate gyrus, hippocampus, and subicular complex. *J Comp Neurol* 307: 434-459.

Witter MP, Groenewegen HJ, Lopes da Silva FH, and Lohman AHM (1989) Functional organization of the extrinsic and intrinsic circuitry of the parahippocampal region. *Prog Neurobiol* 33: 161-254.

Witter MP, Wouterlood FG, Naber PA, and Van Haefern T (2000) Anatomical organization of the parahipocampal-hipocampal network. *Ann N Y Acad Sci* 911: 1-24.

Wyss JM and Van Groen TV (1992) Connections between the retrosplenial cortex and the hippocampal formation in the rat: a review. *Hippocampus* 2: 1-12.

[Received May 2, 2003; accepted June 30, 2003]